

Accepted Manuscript

Title: Exosomes populate the cerebrospinal fluid of preterm infants with post-haemorrhagic hydrocephalus

Authors: Robert Spaul, Bryony McPherson, Andriana Gialeli, Aled Clayton, James Uney, Axel Heep, Óscar Cordero-Llana



PII: S0736-5748(18)30305-8
DOI: <https://doi.org/10.1016/j.ijdevneu.2019.01.004>
Reference: DN 2330

To appear in: *Int. J. Devl Neuroscience*

Received date: 31 October 2018
Revised date: 17 December 2018
Accepted date: 6 January 2019

Please cite this article as: Spaul R, McPherson B, Gialeli A, Clayton A, Uney J, Heep A, Cordero-Llana Ó, Exosomes populate the cerebrospinal fluid of preterm infants with post-haemorrhagic hydrocephalus, *International Journal of Developmental Neuroscience* (2019), <https://doi.org/10.1016/j.ijdevneu.2019.01.004>

This is a PDF file of an unedited manuscript that has been accepted for publication. As a service to our customers we are providing this early version of the manuscript. The manuscript will undergo copyediting, typesetting, and review of the resulting proof before it is published in its final form. Please note that during the production process errors may be discovered which could affect the content, and all legal disclaimers that apply to the journal pertain.

Exosomes populate the cerebrospinal fluid of preterm infants with post-haemorrhagic hydrocephalus

Robert Spaul^{a#}, Bryony McPherson^{a#}, Andriana Gialeli^a, Aled Clayton^b, James Uney^a, Axel Heep^{a,c*}, Óscar Cordero-Llana^a

^a Regenerative Medicine Laboratory, Bristol Medical School, University of Bristol, UK

^b Division of Cancer & Genetics, School of Medicine, University of Cardiff, UK

^c Neonatal Neurology Group, Bristol Medical School, University of Bristol, UK

These authors contributed equally to this work

* Corresponding author, present address:

Professor Axel Heep

University of Oldenburg

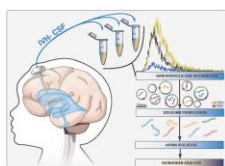
Department of Paediatrics

Germany

Email: axel.heep@bristol.ac.uk

Phone: +44 (0) 117 4146814

Graphical abstract



Highlights:

- Exosomes populate the cerebrospinal fluid of preterm infants with post-haemorrhagic hydrocephalus
- Exosomes found after intraventricular hemorrhage are from serum and brain
- Micro-RNAs isolated from the exosomal fraction relate to development and disease

Abstract

Background

Preterm infants are at risk of germinal matrix haemorrhage-intraventricular haemorrhage (GMH-IVH) which leads to post-haemorrhagic hydrocephalus (PHH) in 30% of infants; this is associated with moderate-severe neurodevelopmental impairment and confers significant risk of cerebral palsy. There are however no predictive indicators of the severity or long-term outcome after GMH-IVH. In recent years, endosome-derived extracellular vesicles (EVs) or exosomes have been isolated from biofluids and shown to mediate intercellular communication via selective enrichment in proteins and micro-RNAs.

Methods

This study aimed to isolate and characterise EVs from the cerebrospinal fluid (CSF) of 3 preterm infants with PHH using nanoparticle tracking analysis (NTA), transmission electron microscopy (TEM) with immunogold protein labelling, and micro-RNA analysis.

Results

NTA of unaltered CSF revealed a heterogeneous and dynamic population of EVs. Exosomal-sized EVs were isolated by differential ultracentrifugation and TEM confirmed the presence of CD63⁺ and CD81⁺ exosomes. The micro-RNAs miR-9, miR-17, miR-26a, miR-124 and miR-1911 were detected within the exosome-enriched fraction and profiled over time.

Conclusion

This is the first reported characterisation of exosomes from the CSF of preterm infants with post-haemorrhagic hydrocephalus.

Keywords: Exosome; Preterm infant; Cerebrospinal fluid; Intraventricular hemorrhage; Cerebral palsy; Micro RNA

1 Background

Preterm infants (<32 weeks gestational age) are at risk of a serious brain injury, called germinal matrix haemorrhage - intraventricular haemorrhage (GMH-IVH). GMH-IVH most commonly occurs in the first 48h after birth¹ and is thought to arise from rupture of the capillaries of the subependymal germinal matrix². Despite improved neonatal care leading to better survival, the incidence of GMH-IVH has remained static³. Post-haemorrhagic hydrocephalus (PHH) is a serious complication of GMH-IVH and aspiration from a ventricular access device is used to relieve the excess cerebrospinal fluid (CSF) from the ventricles. GMH-IVH can lead to many moderate to serious comorbidities, such as cerebral palsy⁴. To date we lack predictive indicators to identify the level of the damage or the long-term outcomes of GMH-IVH.

However, in recent years, exosomes isolated from body fluids have emerged as reservoirs of sensitive biomarkers.

Exosomes are spherical cell-derived vesicles between 30-100nm in diameter⁵. The earliest evidence of exosomes came in the 1980s when the vesicular release of the intact transferrin receptor from maturing reticulocytes was observed *in vitro*⁶. Exosomes are produced by almost all cell types including neurons, microglia, and dendritic cells in the CNS⁷. Exosomes fall under the category of extracellular vesicles (EV) which also includes microvesicles (also known as ectosomes) and apoptotic bodies^{7,8}. Their key difference is their mode of biogenesis and several features are used to identify them: Exosomes are actively released by cells as a product of the endocytic pathway and are typically considered to be 30-100nm in diameter; microvesicles are a product of, probably passive, plasma membrane budding and range from 50-1000nm; while apoptotic bodies, a product of apoptosis, are typically 50-5000nm^{5,6,8,9}. Aside from size, exosomes differ in their selective enrichment in certain proteins including tetraspanins CD63, CD81, and CD9¹⁰⁻¹³.

Interest in exosomes has grown rapidly and they are now recognised as sophisticated means of long and short distance intercellular communication⁹. Systemic inflammation has been shown to increase the release of extracellular vesicles by the choroid plexus epithelium. These vesicles contain pro-inflammatory factors - including microRNAs- that directly cause the activation of astrocytes and microglia in the brain parenchyma¹⁴. Exosomes in the embryonic CSF have also been shown to modulate IGF signalling and promote Neural Stem Cell proliferation (NSC)¹⁵. Exosomes have been proposed as promising non-invasive diagnostic tools for

cancer¹⁶, kidney diseases¹⁷ and neurodegeneration^{18,19} but have not been explored in neonatal development and GMH-IVH/PHH.

2 Methods

2.1 Diagnosis of PHH and CSF collection

CSF was collected from preterm infants born at less than 32 weeks gestation treated for evolving posthaemorrhagic hydrocephalus (PHH) admitted to the regional Neonatal Intensive Care Unit at Southmead Hospital in Bristol, United Kingdom. Intraventricular haemorrhage (IVH) was diagnosed on routine trans-fontanel cranial ultrasound studies (CUSS). Subsequent CUSS were performed 1-3 times a week in order to follow progression of GMH-IVH and development of PHH. The diagnosis and treatment of PHH was indicated by the ultrasound measurement of ventricular index (VI) and anterior horn width (AHW) according to Levene & Sartre²⁰. External CSF drainage was indicated by VI and AHW exceeding 97th percentile and initially undertaken via lumbar puncture before insertion of a ventricular access device (VAD) if ventricular enlargement persisted above the 97th percentile (Department of Paediatric Neurosurgery, Bristol Royal Hospital for Children, Bristol, United Kingdom).

CSF used in this study was the excess fluid remaining after routine testing of samples taken for clinical indications following informed parental consent. Initial sample volume was 10mL/kg body weight, the mean volume per sample available for testing was 4.4mL. Ethical approval for analysis of the CSF was obtained from NHS Research Ethics Committee (REC number: 15-YH-0251). From each patient, CSF was collected at different time points. CSF was centrifuged to remove cellular material and the

supernatant frozen at -20°C within an hour of collection, with transfer to -80°C as soon as practicable. Patients with suspected CNS infection (defined as raised WCC or positive bacterial culture in the CSF), known genetic abnormalities, or presenting with CNS malformation were excluded from the study. Patients and samples used in this study are indicated in Table S1.

2.2 Nanoparticle Tracking Analysis

Unprocessed CSF nanoparticle size distribution and concentration was determined using the NanoSight NS300 (Malvern, Amesbury, UK). CSF was diluted in distilled water (final volume 1ml) to ensure an appropriate concentration of particles detectable by the instrument. Each sample was analysed in triplicate using video recordings each 3 minutes in duration.

2.3 Differential ultracentrifugation

Exosome isolation was based on the method described by Théry et al ²¹ and took place at 4°C unless otherwise stated. CSF was thawed in 1.5ml Eppendorf Tubes, vortexed, then centrifuged at 2000g for 10min, then again at 10,000g for 20min to pellet dead cells and cell debris. The supernatant was then transferred into 1.5ml Beckman Ultracentrifuge Tubes (Beckman Coulter, London, UK) and ultracentrifuged in a fixed angle TLA-55 rotor (Beckman Coulter, London) at 100,000g (40,000 rpm) for 70min to pellet the exosomes. If a washing step was required, the exosome-enriched pellet was resuspended in PBS and ultracentrifuged as above. The pellet was resuspended in 100 μl of filtered PBS and stored at -80°C until further analysis. Repeat freeze-thaw cycles (> 2) were avoided. For a flow diagram of this method see Figure S1.

2.4 exoEasy Maxi Kit extracellular vesicle purification

CSF was thawed in 1.5ml Eppendorf Tubes and vortexed. All spin columns, collection tubes, and reagents were supplied in the exoEasy Maxi kit (Qiagen, Manchester, UK) and isolation was performed according to the manufacturer's instructions. Briefly, CSF from each patient was added to Buffer XBP (1:1), mixed thoroughly, and allowed to reach room temperature. This was centrifuged through an exoEasy spin column (max 16ml/column) at 500g for 1min. Flow-through was discarded and the column washed through with 10mL buffer XWP centrifuged at 5,000g for 5min. The flow-through was discarded and 400µl Buffer XE was added to the spin column, incubated at room temperature for 1min, then centrifuged at 500g for 5min, then again with the same eluate at 5,000g for 5min (Figure S1) and the final eluate (400µl) was stored at -80°C until RNA extraction.

2.5 Transmission electron microscopy

Negative staining was adapted from a previously described method²². If immunogold labelling did not occur, 2µl of the EV-enriched sample was placed on a carbon-coated formvar film on a copper grid (300 mesh) (Agar Scientific, Stansted, UK) and left for 1 min. For all samples the grid was washed on a droplet of distilled water for 10sec prior to incubation in uranyl acetate (3% in dH₂O) (BDH Industries, Mumbai, India) and methyl cellulose (2% in dH₂O) (Sigma Aldrich) mixed in a ratio of 1:9 for 5min on ice. Using a loop to remove excess fluid, the grid was dragged across a Whatman 1 filter (GE Healthcare, Buckinghamshire, UK) and left to air-dry upright.

Immunogold labelling was adapted from a previously described method²². All incubations occurred at room temperature unless otherwise stated. Following exosome isolation 2µl of sample were placed onto a carbon-coated formvar film on a

copper grid (300 mesh) (Agar Scientific, Stansted, UK) and left for 2min. Grids were fixed and blocked by incubation for 5min per step on a drop of 1% paraformaldehyde (PFA) (Sigma Aldrich, Irvine, UK), then 50nM glycine in PBS (Gibco), followed by 0.1% bovine serum albumin (BSA-c) (Aurion, The Netherlands). Grids were then incubated with the selected primary antibody: anti-CD63 mAb (100µg/ml) or anti-CD81 mAb (200µg/ml) (both diluted 1:50 in 0.1% BSA and both Santa Cruz Biotechnology, Heidelberg, Germany) and left for at least 30min. Grids were washed 3 times in 0.1% BSA to prevent secondary staining, allowing 5min between washes, then incubated on a drop of secondary gold-conjugated goat anti-mouse IgG (Aurion) (6nm) (diluted 1:20 in 0.1% BSA/PBS) and left for at least 30min. Grids were washed 3 times and negatively stained as above.

All Grids were viewed and photographed using a FEI Tecnai™ 12 transmission electron microscope and images analysed using ImageJ.

2.6 Exosome size distribution measurements

15 randomly-taken electron micrographs per sample were analysed in ImageJ. EVs were identified as spherical/cup-shaped particles with the presence of a surrounding continuous membrane and the Feret's diameter of each EV was determined.

2.7 RNA extraction

Total RNA was extracted from EVs using the mirVana™ miRNA Isolation Kit (Ambion) according to the manufacturer's instructions using reagents included in the kit. 500µl lysis/binding solution were added directly to pelleted exosomes to maximise RNA yield, then vortexed to lyse the exosomes. miRNA Homogenate Additive was added (1/10 the volume of the exosome lysate), vortexed, and incubated on ice for 10min.

500µl Acid-Phenol:Chloroform was added and vortexed, then centrifuged at 10,000g for 5min at room temperature (Eppendorf centrifuge 5430R). The upper aqueous phase was carefully removed and transferred to a fresh 1.5ml Eppendorf tube and x 1.25 volumes of 100% ethanol (Sigma Aldrich) was added. This mixture was passed through a Filter Cartridge by centrifuging at 10,000g for 15sec, and the Filter Cartridge washed with 700µl miRNA Wash Solution 1 by centrifuging at 10,000g for 15sec. This step was repeated twice with 500µl Wash Solution 2/3 with a final spin at 10,000g for 1min. The contents were eluted by passing 100µl of nuclease-free water (pre-heated to 95°C) through the Filter Cartridge and spun at maximum speed for 20-30sec. The eluate, containing total RNA, was stored at -20°C until further analysis. Total RNA concentration was measured using the Nanotube 2000 spectrophotometer (Thermo Fisher).

2.9 Candidate miRNA selection

miRNAs were selected based on their enrichment in specific fractions of CSF/serum. This was based on a recent report by Yagi *et al.* (2017) who performed next generation sequencing of exosomal miRNAs within adult human CSF²³.

2.10 qRT-PCR

Reverse transcription (RT) and real-time PCR (qPCR) were performed using the TaqMan® MicroRNA Assay according to the manufacturer's instructions (Applied Biosystems™, ThermoFisher). Single-stranded cDNA was synthesized using miRNA-specific RT looped-primers (5X). Each 10µl RT reaction contained 6ng/ml total RNA. Using the cDNA products from above, qPCR was performed using sequence-specific primers and the TaqMan® Universal Master Mix II, containing no uracil *N*-glycosylase (UNG) (Applied Biosystems). qPCR was performed in triplicates on a StepOnePlus™

real-time PCR system (Applied Biosystems) to detect mature miRNA expression. As there are no housekeeping RNAs yet identified within exosomes the results shown are expression relative to the first time point for each miRNA.

2.11 Data Analysis

Data were analysed using GraphPad Prism 6. Graphs were plotted \pm SD or \pm SEM as appropriate as specified in figure legends.

3 Results

3.1 CSF of preterm infants with PHH contains exosomes

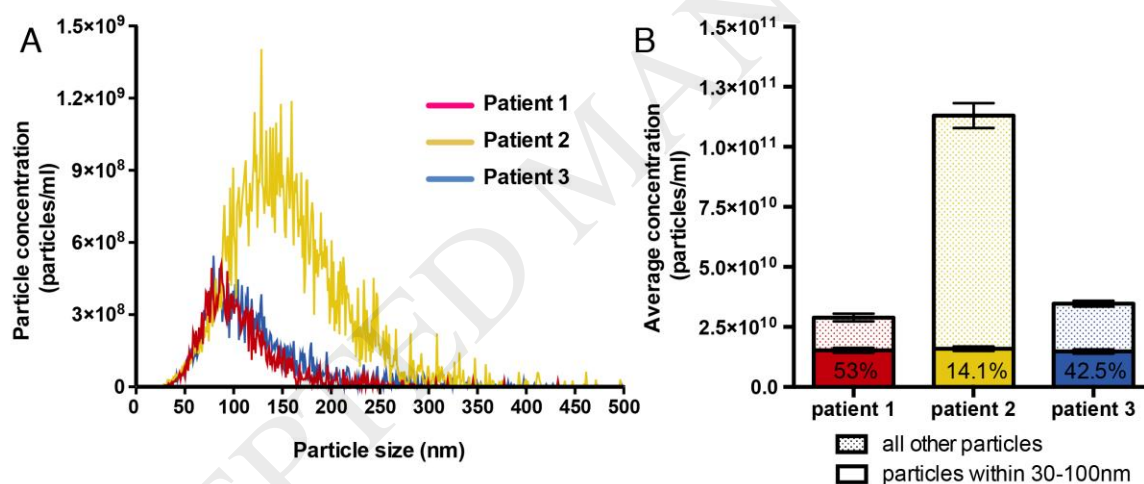


Figure 1 **A)** Nanoparticle tracking analysis of CSF from three patients with PHH. 120-second videos were recorded for each patient and concentrations taken as an average of triplicate runs. Lines show the concentration of particles at a given size within whole CSF \pm SEM. Data is processed with the finite track length adjustment algorithm on the NanoSight NS300 software. **B)** Concentration of particles detected in whole CSF, quantified using NTA. The shaded region of the bar indicates the concentration of particles within 30-100nm range out of all particles detected.

Nanoparticle tracking analysis (NTA) is a widely used technique in the EV field to accurately determine the size distribution and concentration of nanoparticles in

fluids, based on the principle of Brownian motion²⁴. We performed NTA on CSF from three patient samples to determine whether nanoparticles the size of exosomes (30-100nm) were present. Figure 1 (A) demonstrates there is a heterogeneous population of particles within CSF, and that this varies between patients. The mean particle size was 106.9 ± 0.44 nm, 156.9 ± 2.08 nm, and 120.77 ± 1.2 nm for patients 1, 2, and 3 respectively. The modal particle sizes for patients 1 and 3 were similar: 86.2nm and 81.9nm while the modal particle size in patient 2 was 159.3nm. Different particle concentrations were observed across the three patients: $2.89 \times 10^{10} \pm 9.17 \times 10^8$; $1.13 \times 10^{11} \pm 3 \times 10^9$ and $3.47 \times 10^{10} \pm 6.96 \times 10^8$ particles/ml for patients 1, 2, and 3 respectively. The concentration of particles that fit the size criteria for exosomes was similar across all three patients: $1.53 \times 10^{10} \pm 5.83 \times 10^8$; $1.59 \times 10^{10} \pm 5.29 \times 10^8$ and $1.48 \times 10^{10} \pm 5.15 \times 10^8$ particles/ml were within 30-100nm for patients 1, 2 and 3 respectively. It is likely that this represents a low estimate for small-EV concentration as, due to the limits of refraction, this analysis under-samples small vesicles (<45nm). Interestingly, although CSF from patient 2 contained the highest total concentration of particles, only 14.1% was within the exosomal range compared to 53% and 42.5% in patient 1 and patient 3 respectively (Figure 1 (B)).

3.2 CSF particle profiling over the course of four months following PHH

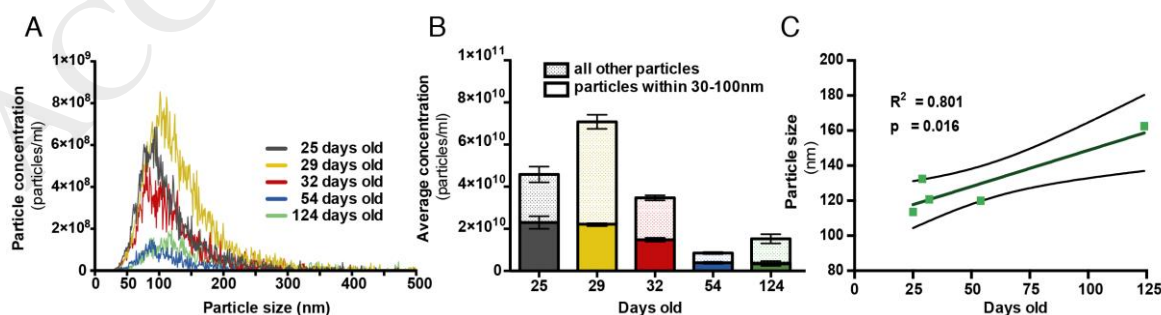


Figure 2 A) Nanoparticle tracking analysis of CSF nanoparticles from patient 3 over the course of four months. 120-second videos were recorded for each sample and concentrations taken as an average of triplicate runs. Lines show the concentration of particles at a given size within whole CSF \pm SEM. Data is processed with the finite track length adjustment algorithm on the NanoSight NS300 software. **B)** Concentration of particles detected in whole CSF, quantified using NTA over the course of four months. The shaded region of the bar indicates the concentration of particles within 30-100nm range out of all particles detected. **C)** Regression analysis showing positive correlation between days post PHH and mean extracellular vesicle size in CSF.

To further this characterisation, we focused on patient 3 as CSF samples were obtained throughout the treatment course. NTA of whole CSF taken at five time points revealed the heterogeneous population of EVs within CSF (Figure 2 (A)). Exosome-sized particles were detected in all samples of CSF. At 25, 32 and 54 days old the modal particle sizes were within the range of exosomes (83.6nm, 81.9nm and 85.4nm respectively). At 29 and 124 days the modal particle size was above the size criteria for exosomes (104.6, and 122.6nm respectively). The mean particle sizes were 113.60 ± 1.70 nm, 132.40 ± 1.82 nm, 120.77 ± 1.82 nm, 119.3 ± 3.24 nm, 135.25 ± 0.55 nm, and 162.60 ± 1.57 nm for 25, 29, 32, 54, and 124 days. Interestingly, both the overall particle concentration and the proportion of particles within 30-100nm range appear to show a gradual decrease with the GMH-IVH treatment progression (Figure 2 (B)). While the mean ($R^2=0.801$, $p=0.016$) and modal ($R^2=0.744$, $p=0.027$) particle size increases with time following PHH (Figure 2 (C)).

3.3 CD63⁺ and CD81⁺ exosomes are present in the CSF of premature infants following PHH

NTA cannot distinguish between EVs and similar sized particles which lack a lipid membrane, therefore we used TEM to qualitatively characterize these vesicles. We compared three isolation methods. Differential ultracentrifugation is the original protocol used to isolate exosomes, described by Raposo et al., 1996²⁵. Ultracentrifugation followed by a washing step is suggested by Théry et al (2006)²¹ as a means of removing contaminating proteins, although it has been reported to result in a reduced exosomal yield²⁶. The commercially available exoEasy Maxi Kit isolates EVs using a spin-column system whereby EVs bind to an affinity membrane based on the presence of vesicular biochemical features. Exosome purification using this kit takes under 30min. Following exosome isolation, the final eluates were negatively stained for TEM. EVs were observed under electron microscopy in all three patients with all purification methods. These had the characteristic spherical shape with a lipid bilayer and corresponded to the size of exosomes (30-100nm) (Figure 3 (A-C)). Of note, following isolation via the exoEasy kit, the final eluate appeared cloudy and large precipitates were observed under electron microscopy (Figure S2).

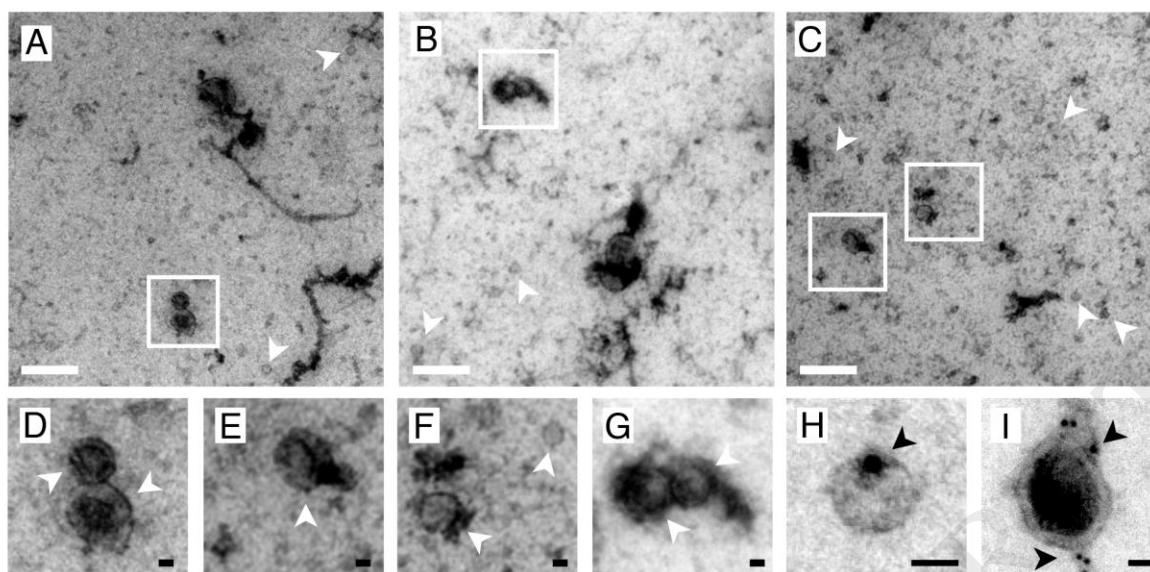


Figure 3: Transmission electron micrographs of extracellular vesicles isolated from the CSF of three patients following differential ultracentrifugation. Samples were negatively stained with uranyl acetate. A-C (patients 1-3 respectively) show cup-shaped membranous vesicles within the size range of exosomes, indicated by white arrowheads. Insets (D-G) show zoomed in area of probable exosomes. H and I show positive immunogold labelling for CD63 and CD81 (6nm gold particles) from patient 3. CSF samples were aspirated from the patient at 75 days old. White scale bars indicate 100nm, black scale bars 20nm.

CD63 and CD81 are surface tetraspanins widely used as markers for exosomes ²⁷. Following exosomal isolation of CSF, we stained the exosome-enriched fraction using immunogold labelling techniques and anti-CD63/anti-CD81 antibodies. Colloidal gold particles, shown as small black dots in Figure 3 (H-I) indicated positive labelling for both tetraspanins on the surface of nanoparticles within the size range and morphology of exosomes. To determine the size distribution of EVs isolated from the CSF, imaged electron micrographs were viewed in ImageJ and EVs manually counted. A total of 265 EVs were counted across the 3 patients, which ranged from 23.1nm to 214.9nm in diameter. For patients 1-3, the modal particle sizes were 42.5nm ($\bar{x}=53.5\pm 23.8\text{nm}$), 42.5nm ($\bar{x}=75.5\pm 39.2\text{nm}$) and 32.5nm ($\bar{x}=42.1\pm 18.5\text{nm}$) respectively (Figure S3). All modal particle sizes were within 30-100nm suggesting

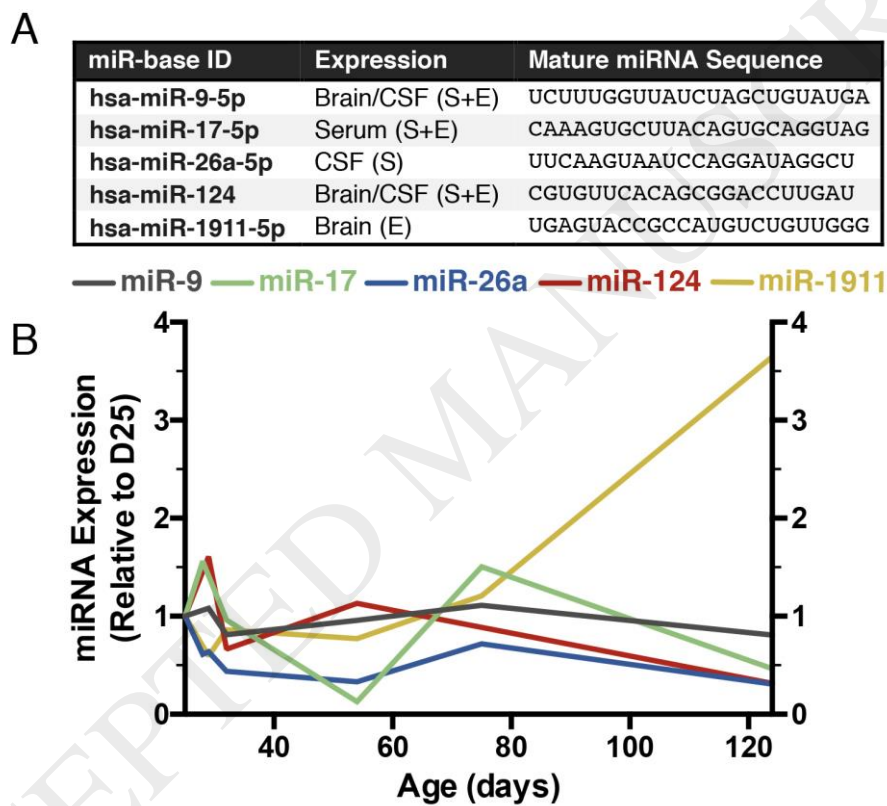
that the majority of nanoparticles purified following exosome isolation are within the size range of exosomes. As expected, larger particles are removed by the 10,000 g spin and therefore both modal and mean particle sizes following purification were lower than the original values obtained with NTA.

3.4 The exosome-enriched fraction of CSF contains miRNA

ACCEPTED MANUSCRIPT

After demonstrating the presence of exosomes in CSF, based on morphology, size and positive immunogold labelling, we aimed to isolate exosomal RNA. Following exosome isolation, total RNA was extracted from all samples. Ultracentrifugation and ultracentrifugation with a washing step yielded similar levels of RNA at $0.2\pm 0.004\text{ng}/\mu\text{l}$ and $0.16\pm 0.042\text{ng}/\mu\text{l}$ respectively. Exosome isolation using the exoEasy kit yielded the most RNA at $0.47\pm 0.324\text{ng}/\mu\text{l}$, but final RNA concentrations were remarkably variable (Figure S4). To determine whether exosomal miRNAs are present in the CSF of patients with infantile PHH, five miRNAs (previously shown to be present in CSF/serum²³) were selected and quantified by qPCR. These miRNAs were miR-17 (serum-specific), miR-26a (highly expressed in CSF exosomes), miR-124 (brain-specific), miR-9 (brain specific and known regulator of neurogenesis²⁸) and miR-1911 (brain specific, highly enriched in CSF exosomes). Mature miRNA sequences are detailed on Figure 4 (A). All five miRNAs were detectable in the

exosome-enriched fraction of CSF. miR-9 and miR-26a levels were relatively constant over the course of four months following PHH. Interestingly, we observed a decrease in expression levels of miR-17 and miR-124 at the latest time point (124 days after birth) relative to the earliest time point (25 days after birth). Conversely miR-1911 expression showed a general increase over the four months following PHH (Figure 4 (B)).



Figure

1 of the μ RNA selected for this study. E: μ RNA detected in exosomes, S: μ RNA detected in cell supernatant. **B)** Relative expression of five miRNAs over four months quantified using qPCR. CSF samples from patient 3 was ultracentrifuged at 100,000 g (section 3.3.1). RNA was isolated from the exosome-enriched pellet using the mirVana™ miRNA Isolation Kit and reverse transcription and qPCR performed using the TaqMan® MicroRNA Assay. Expression of each miRNA was normalised to the starting volume of CSF and relative to the earliest CSF acquisition time point.

4 Discussion

Our first aim was to confirm the presence of exosomes in the CSF of our patient cohort, as exosomes had been previously documented in human adult CSF²⁹. Our NTA data of whole PHH-CSF suggested the presence of exosomes, apoptotic bodies, and microvesicles in all samples for all three of our patients. The concentration of EVs in CSF is an order of magnitude lower than in the serum, with typical concentrations of 1.1×10^{10} particles/mL²⁹. We then profiled the concentrations of each patient sample and the relative number of particles within the exosomal range. Patient 2 had a much higher particle concentration and contained a larger proportion of particles >100nm compared to patients 1 and 3, suggesting a higher concentration of microvesicles or apoptotic bodies in this patient. Interestingly, Georgiadis et al. 2008 reported an inflammatory response in a rabbit model of GMH-IVH with an increased number of apoptotic cells in the periventricular zone of the brain compared to a control group without GMH-IVH³⁰. Therefore, a larger proportion of apoptotic bodies in patient 2 could indicate a greater ongoing inflammatory response. However, whether the number of apoptotic bodies present in PHH-CSF impacts the future prognosis in these patients remains to be investigated.

Following the confirmation that exosome-sized nanoparticles were present in PHH-CSF, we sought to further characterise them using TEM since NTA cannot distinguish between exosomes and similarly sized particles which lack a membrane. TEM revealed spherical vesicles with a continuous membrane that were CD63⁺ and CD81⁺ supporting the presence of exosomes in PHH-CSF. However, it is important to keep in mind that one of the primary limitations in

the exosome field is the lack of a definitive marker and that none of the reported proteins (including CD63 and CD81) are completely exclusive to exosomes. TEM quantification also demonstrated that there is a heterogeneous population of nanoparticles in PHH-CSF even after exosome isolation. This heterogeneity is in agreement with Willms et al., 2016 who demonstrated the presence of two distinct exosome subpopulations within the culture media of 4 different cell types. These subpopulations had different modal sizes, protein content, RNA composition and different functional effects on recipient cells³¹. We then profiled nanoparticle composition over a four-month time period following PHH. NTA revealed a general decrease in the concentration of exosome-sized nanoparticles over the course of four months following PHH. Interestingly Tietje et al., 2014 have reported a similar temporal decline in the concentration of CSF EVs over the course of 85 years³² suggesting that this may be of biological significance. However, further investigation is needed to ascertain whether the decline in CSF particle concentration is specific to PHH, or occurs as a consequence of perinatal development.

We then attempted to isolate exosomal RNA from our CSF samples. Following RNA isolation, we used qPCR to determine the presence of exosomal miRNAs. Due to the low yield of RNA and limited sample volumes, we focused on a small panel of miRNAs selected on the basis of their presence in CSF and serum fractions. miR-17, miR-26a, miR-124, miR-1911 and miR-9 were detectable in PHH-CSF albeit at low expression levels. This is in line with the stoichiometric analysis of biofluid samples and *in vitro* cultures performed by Chevillet et al., that found only ~1 miRNA to every 121 exosomes³³. We then hypothesised that exosomal miRNA expression might change over time following GMH-IVH, as

such, we performed qPCR on a panel of five miRNAs. miR-9 is an important regulator of neurogenesis, involved in coordinating both differentiation and proliferation of NSCs^{34,35}. miR-26a has been shown to induce neurite outgrowth in rats; an essential process during neuronal migration and differentiation during development³⁶. Expression of both miR-9 and miR-26a remained constant over the four months following PHH. This was unexpected considering their implications in neuronal development but suggest that they would not be suitable biomarkers for GMH-IVH progression. miR-17 is a serum-specific miRNA²³. We observed a negative correlation between miR-17 and time following PHH. Disruption of the blood brain barrier (BBB) and/or direct bleeding at the time of injury in GMH-IVH, leads to serum contamination and therefore abnormal expression of miR-17 in early CSF samples. A progressive reduction of miR-17 CSF levels could reflect restoration of the BBB integrity. miR-124 is a highly conserved and abundantly expressed, brain-specific miRNA³⁷. miR-124 expression has been shown to increase during neuronal development in line with maturation of neurons in a rat model³⁸. However, in our cohort miR-124 expression was negatively correlated with time following PHH which could underpin some of the developmental impairment seen in GMH-IVH patients. miR-1911 was selected as a brain-specific miRNA, found to be highly enriched in CSF exosomes. The increase in miR-1911-5p following GMH-IVH and the development of PHH make this an interesting potential biomarker.

5 Conclusions

To our knowledge, this is the first evidence of exosomes and exosomal miRNA expression in PHH-CSF. We have demonstrated the presence of a heterogeneous population of EVs in PHH-CSF which includes CD63⁺ and CD81⁺ exosomes. We have shown that the exosomal concentration decreases over the course of four months following PHH and that these exosomes contain miRNA that may present themselves as potential biomarkers for PHH. These miRNAs are critical for brain development and therefore may reflect patient responses to treatments or the pathological processes occurring in the development or resolution of PHH.

None of the participating scientists have competing financial interests.

References

- 1 Ballabh, P. Intraventricular Hemorrhage in Premature Infants: Mechanism of Disease. *Pediatr Res* **67**, 1-8, doi:10.1203/PDR.0b013e3181c1b176 (2010).
- 2 Hambleton, G. & Wigglesworth, J. S. Origin of intraventricular haemorrhage in the preterm infant., doi:10.1136/adc.51.9.651 (1976).
- 3 Wilson-Costello, D., Friedman, H., Minich, N., Fanaroff, A. A. & Hack, M. Improved survival rates with increased neurodevelopmental disability for extremely low birth weight infants in the 1990s. *Pediatrics* **115**, 997-1003, doi:10.1542/peds.2004-0221 (2005).
- 4 Vohr, B. R. *et al.* School-age outcomes of very low birth weight infants in the indomethacin intraventricular hemorrhage prevention trial. *Pediatrics* **111**, e340-346 (2003).
- 5 They, C., Zitvogel, L. & Amigorena, S. in *Nat Rev Immunol* Vol. 2 569-579 (2002).
- 6 Harding, C., Heuser, J. & Stahl, P. Receptor-mediated endocytosis of transferrin and recycling of the transferrin receptor in rat reticulocytes. *The Journal of cell biology* **97**, 329-339 (1983).
- 7 Kalra, H. *et al.* Vesiclepedia: a compendium for extracellular vesicles with continuous community annotation. *PLoS biology* **10**, e1001450, doi:10.1371/journal.pbio.1001450 (2012).
- 8 Akers, J. C., Gonda, D., Kim, R., Carter, B. S. & Chen, C. C. Biogenesis of extracellular vesicles (EV): exosomes, microvesicles, retrovirus-like vesicles, and

apoptotic bodies. *Journal of neuro-oncology* **113**, 1-11, doi:10.1007/s11060-013-1084-8 (2013).

9 Cocucci, E. & Meldolesi, J. Ectosomes and exosomes: shedding the confusion between extracellular vesicles. *Trends in cell biology* **25**, 364-372, doi:10.1016/j.tcb.2015.01.004 (2015).

10 Simons, M. & Raposo, G. Exosomes--vesicular carriers for intercellular communication. *Current opinion in cell biology* **21**, 575-581, doi:10.1016/j.ceb.2009.03.007 (2009).

11 Pols, M. S. & Klumperman, J. Trafficking and function of the tetraspanin CD63. *Experimental cell research* **315**, 1584-1592, doi:10.1016/j.yexcr.2008.09.020 (2009).

12 Perez-Hernandez, D. *et al.* The intracellular interactome of tetraspanin-enriched microdomains reveals their function as sorting machineries toward exosomes. *The Journal of biological chemistry* **288**, 11649-11661, doi:10.1074/jbc.M112.445304 (2013).

13 Mittelbrunn, M. *et al.* Unidirectional transfer of microRNA-loaded exosomes from T cells to antigen-presenting cells. *Nature communications* **2**, 282, doi:10.1038/ncomms1285 (2011).

14 Balusu, S. *et al.* Identification of a novel mechanism of blood-brain communication during peripheral inflammation via choroid plexus-derived extracellular vesicles. *EMBO molecular medicine* **8**, 1162-1183, doi:10.15252/emmm.201606271 (2016).

- 15 Feliciano, D. M., Zhang, S., Nasrallah, C. M., Lisgo, S. N. & Bordey, A. Embryonic cerebrospinal fluid nanovesicles carry evolutionarily conserved molecules and promote neural stem cell amplification. *PloS one* **9**, e88810, doi:10.1371/journal.pone.0088810 (2014).
- 16 Skog, J. *et al.* Glioblastoma microvesicles transport RNA and protein that promote tumor growth and provide diagnostic biomarkers. *Nat Cell Biol* **10**, 1470-1476, doi:10.1038/ncb1800 (2008).
- 17 Spanu, S., van Roeyen, C. R., Denecke, B., Floege, J. & Muhlfield, A. S. Urinary exosomes: a novel means to non-invasively assess changes in renal gene and protein expression. *PloS one* **9**, e109631, doi:10.1371/journal.pone.0109631 (2014).
- 18 Liu, C. G., Song, J., Zhang, Y. Q. & Wang, P. C. MicroRNA-193b is a regulator of amyloid precursor protein in the blood and cerebrospinal fluid derived exosomal microRNA-193b is a biomarker of Alzheimer's disease. *Molecular medicine reports* **10**, 2395-2400, doi:10.3892/mmr.2014.2484 (2014).
- 19 Gui, Y., Liu, H., Zhang, L., Lv, W. & Hu, X. Altered microRNA profiles in cerebrospinal fluid exosome in Parkinson disease and Alzheimer disease. *Oncotarget* **6**, 37043-37053, doi:10.18632/oncotarget.6158 (2015).
- 20 Levene, M. I. & Starte, D. R. A longitudinal study of post-haemorrhagic ventricular dilatation in the newborn. *Arch Dis Child* **56**, 905-910 (1981).
- 21 They, C., Amigorena, S., Raposo, G. & Clayton, A. Isolation and characterization of exosomes from cell culture supernatants and biological fluids. *Current protocols in cell biology* **Chapter 3**, Unit 3.22, doi:10.1002/0471143030.cb0322s30 (2006).

22 Hodgson, L., Tavare, J. & Verkade, P. Development of a quantitative Correlative Light Electron Microscopy technique to study GLUT4 trafficking. *Protoplasma* **251**, 403-416, doi:10.1007/s00709-013-0597-5 (2014).

23 Yagi, Y. *et al.* Next-generation sequencing-based small RNA profiling of cerebrospinal fluid exosomes. *Neuroscience letters* **636**, 48-57, doi:10.1016/j.neulet.2016.10.042 (2017).

24 Filipe, V., Hawe, A. & Jiskoot, W. Critical evaluation of Nanoparticle Tracking Analysis (NTA) by NanoSight for the measurement of nanoparticles and protein aggregates. *Pharmaceutical research* **27**, 796-810, doi:10.1007/s11095-010-0073-2 (2010).

25 Raposo, G. *et al.* B lymphocytes secrete antigen-presenting vesicles. *The Journal of experimental medicine* **183**, 1161-1172 (1996).

26 Momen-Heravi, F. *et al.* Current methods for the isolation of extracellular vesicles. *Biological chemistry* **394**, 1253-1262, doi:10.1515/hsz-2013-0141 (2013).

27 Mathivanan, S., Fahner, C. J., Reid, G. E. & Simpson, R. J. ExoCarta 2012: database of exosomal proteins, RNA and lipids. *Nucleic acids research* **40**, D1241-1244, doi:10.1093/nar/gkr828 (2012).

28 Coolen, M., Katz, S. & Bally-Cuif, L. miR-9: a versatile regulator of neurogenesis. *Frontiers in cellular neuroscience* **7**, 220, doi:10.3389/fncel.2013.00220 (2013).

29 Street, J. M. *et al.* Identification and proteomic profiling of exosomes in human cerebrospinal fluid. *Journal of translational medicine* **10**, 5, doi:10.1186/1479-5876-10-5 (2012).

30 Georgiadis, P. *et al.* Characterization of acute brain injuries and neurobehavioral profiles in a rabbit model of germinal matrix hemorrhage. *Stroke* **39**, 3378-3388, doi:10.1161/strokeaha.107.510883 (2008).

31 Willms, E. *et al.* Cells release subpopulations of exosomes with distinct molecular and biological properties. *Scientific reports* **6**, 22519, doi:10.1038/srep22519 (2016).

32 Tietje, A., Maron, K. N., Wei, Y. & Feliciano, D. M. Cerebrospinal fluid extracellular vesicles undergo age dependent declines and contain known and novel non-coding RNAs. *PloS one* **9**, e113116, doi:10.1371/journal.pone.0113116 (2014).

33 Chevillet, J. R. *et al.* in *Proc Natl Acad Sci U S A* Vol. 111 14888-14893 (2014).

34 Zhao, C., Sun, G., Li, S. & Shi, Y. A feedback regulatory loop involving microRNA-9 and nuclear receptor TLX in neural stem cell fate determination. *Nature structural & molecular biology* **16**, 365-371, doi:10.1038/nsmb.1576 (2009).

35 Delaloy, C. *et al.* MicroRNA-9 coordinates proliferation and migration of human embryonic stem cell-derived neural progenitors. *Cell stem cell* **6**, 323-335, doi:10.1016/j.stem.2010.02.015 (2010).

36 Li, B. & Sun, H. MiR-26a promotes neurite outgrowth by repressing PTEN expression. *Molecular medicine reports* **8**, 676-680, doi:10.3892/mmr.2013.1534 (2013).

37 Lagos-Quintana, M. *et al.* Identification of tissue-specific microRNAs from mouse. *Current biology : CB* **12**, 735-739 (2002).

38 Smirnova, L. *et al.* Regulation of miRNA expression during neural cell specification. *The European journal of neuroscience* **21**, 1469-1477, doi:10.1111/j.1460-9568.2005.03978.x (2005).

Acknowledgements

Specific thanks is given to the parents of the infants involved in this study, also to the staff of the neonatal departments involved in their care.

Many thanks for technical assistance provided by Mark Gurney, Judith Mantell; and to Dr Jason Webber for critical advice.

Author Contributions

All authors made significant contributions to conception and design, acquisition of data, or analysis and interpretation of data. All authors contributed to drafting or revising the article for important intellectual content. All authors approved the final version of the article to be published.

Statement of Financial Support

This work was supported by the David Telling Charitable Foundation, the Elizabeth Blackwell Institute for Health Research, University of Bristol, the Wellcome Trust Institutional Strategic Support Fund, and the Castang Foundation.

Declaration of interest

The authors declare no conflict of interest.